ELSEVIER

Brain Research 723 (1996) 46–60

BRAIN RESEARCH

Research report

Chaotic and phase-locked responses of the somatosensory cortex to a periodic medial lemniscus stimulation in the anesthetized rat

Satoru Ishizuka [a,*], Hatsuo Hayashi [b]

[a] *Department of Physiology, Faculty of Dentistry, Kyushu University, Fukuoka 812, Japan*

[b] *Department of Computer Science and Electronics, Faculty of Computer Science and Systems Engineering, Kyushu Institute of Technology, Iizuka 820, Japan*

Accepted 7 February 1996

Abstract

Field potential responses of the somatosensory cortex to a periodic medial lemniscus (ML) fiber stimulation were investigated in anesthetized rats. Since the field potential responses of the cortex depend on the depth of anesthesia, two criteria were introduced to control the depth of anesthesia. One criterion is that spindle oscillations are caused by a single shock to ML fibers, and the other is that the dominant frequency of spontaneous field potential rhythm is in the frequency range of the delta wave. Phase-lockings and chaotic responses occurred depending on stimulus parameters under the above conditions. Trajectories of the chaotic responses in the two-dimensional phase space (V, dV/dt) reconstruct strange attractors, and stroboscopic cross-sections of each attractor show stretching and folding process. Each one-dimensional strobomap of the chaotic responses is a noninvertible function with an unstable fixed point. This is undoubted evidence for chaotic responses of the somatosensory cortex in vivo. Power spectra well characterize the periodic and the chaotic responses. Positive Lyapunov exponents and low, noninteger correlation dimensions of the chaotic responses are consistent with the above evidence. Consequently, four kinds of chaotic responses were classified. A periodic–chaotic transition sequence was observed at a relatively low stimulus current when the frequency of the stimulation was varied. A cascade of period-doubling bifurcations was also observed on a route from the region of the 1:1 phase-locking to one of the regions of the chaotic responses.

Keywords: Somatosensory cortex; Anesthetized rat; Periodic medial lemniscus stimulation; Field potential; Phase-locking; Chaos; One-dimensional strobomap; Strange attractor; Period doubling-bifurcation; Correlation dimension; Lyapunov exponent

1. Introduction

When peripheral receptors are stimulated by sensory stimuli, trains of action potentials are generated in afferent nerves due to generator potentials. In other words, sensory information such as intensity and modality of the stimulation is transformed into the frequency of impulses and the number of activated afferent fibers. The trains of impulses are quite periodic. How does the central nervous system (CNS) respond to such periodic impulses? The brain consists of active, nonlinear elements, namely neurons, and some kinds of neurons show spontaneous, rhythmic activity. Therefore, the brain would cause complex responses to a periodic input: for example, phase-lockings and chaotic responses. In fact, fluctuations and augmentation of field potential responses of the somatosensory cortex are caused by a periodic thalamic nucleus stimulation in the 6–10 Hz range [30,31,37]. Moreover, vibrissa cortex neurons in paralyzed cats are unable to follow a periodic afferent nerve stimulation in the frequency range above 30 Hz [23].

Electroencephalogram (EEG) data show rhythmic activities which correspond to behavioral states of the animal: for example, delta and theta waves during sleep, and alpha and beta waves during awakening. Stimulus-specific synchronized oscillations in the high frequency range (30 to 80 Hz) have also been observed in several visual cortical areas of awake animals [9,10,13,16,27]. Larger amplitude of such rhythmic EEG activity reflects better synchronization of neuronal activities, and epileptic EEGs are observed in the case of an exceeding synchronization. These suggest that activities of many cortical neurons synchronize with each other in proper conditions. Therefore, it has been supposed that EEGs of the mammalian brain observed at various behavioral states can be described as behavior of a dynamical system with small degrees of

* Corresponding author. Fax: (81) (92) 641-3770; E-mail: sishidec@mbox.nc.kyushu-u.ac.jp

PII S0006-8993(96)00214-4

freedom. Actually, low correlation dimensions of alpha and beta rhythms [2,3,8], EEGs at sleep stages [2] and petit mal epilepsy [3] have been estimated. Moreover, it has been suggested that the EEGs are chaotic because of the non-integer correlation dimensions. However, the problem of the Grassberger and Procaccia's algorithm to estimate the correlation dimension has been indicated [33,48], and the degrees of freedom of the EEGs are still controversial. Recently, the algorithm has carefully been used to investigate dynamical features of EEGs. For example, the surrogate algorithm has been developed [36,48]. Surrogate data are stochastic time series whose linear correlation characteristics are the same as those of the real data. When the correlation dimensions of real and surrogate data are different it may be concluded that the real data are non-random. However, this procedure does not provide evidence for chaos. Moreover, Acherman et al. have demonstrated that all-night sleep EEG signals and randomized control signals with the identical power spectra have similar correlation dimensions [1]. On the other hand, the largest Lyapunov exponents of EEGs have also been estimated [2,11,12,43]. However, the Lyapunov exponents of the real EEG signals are problematic because of finite epochs of EEG signals and finite signal to noise ratio.

Responses of several pacemaker neurons to a periodic input have been investigated in computer-simulations [6,35] and experiments [17–21,35,40]. These response patterns depend on the intensity and/or the frequency of periodic input, and pacemaker neurons cause phase-lockings and chaotic responses in proper conditions. For example, chaotic features of irregular responses of the *Onchidium* pacemaker neuron have been demonstrated by one-dimensional strobomaps, and three kinds of chaotic responses have been illustrated [19,20]. These studies are important to understand the complexity of the responses from a viewpoint of deterministic dynamics.

We have recently reported that irregular responses of hippocampal CA3 slices to a mossy fiber stimulation are obviously chaotic [22]. The chaotic responses show broadband spectra, and their trajectories in a three-dimensional phase space reconstruct strange attractors. Moreover, one-dimensional strobomaps are noninvertible functions with an unstable fixed point. However, the experimental conditions were not normal, and the hippocampal CA3 was not functional, because the slices were perfused with the medium containing 2 mM penicillin and 8 mM K^+ in order to generate spontaneous epileptiform oscillations in CA3. Therefore, it is desired to obtain undoubted evidence for chaos in normal functioning brain and to show relationships between chaos and information processing in the brain. In this paper, responses of the somatosensory cortex in anesthetized rats to a periodic medial lemniscus (ML) stimulation were investigated.

Phase-lockings and chaotic responses occurred in some regions of stimulus parameters. Trajectories of the chaotic responses reconstruct strange attractors in a two-dimensional phase space, and stroboscopic cross-sections of each attractor show stretching and folding process. Each one-dimensional strobomap of the chaotic responses is a noninvertible function with an unstable fixed point. This is undoubted evidence for chaotic responses of the somatosensory cortex in vivo. Consequently, four kinds of chaotic responses are illustrated. Positive Lyapunov exponents and low noninteger correlation dimensions estimated from the chaotic responses support the above evidence. A periodic–chaotic transition sequence was observed at a relatively low stimulus current when the frequency of the stimulation was varied. A cascade of period-doubling bifurcations was also observed on a route from the 1:1 phase-locking to a kind of the chaotic responses. The relevance of the chaotic responses to handling of sensory information will be discussed.

2. Materials and methods

2.1. Experimental methods

Experiments were performed using fourteen adult Wistar rats of both sexes (body weight: 280–440 g) that were obtained from a local breeder (Seiwa Experimental Animals, Fukuoka). The guiding principles for care and use of animals in the field of physiological sciences outlined by the Physiological Society of Japan were followed carefully. The rats were anesthetized with urethane (1–1.4 g/kg, i.p.) or pentobarbital (60–90 mg/kg, i.p.), and mounted on a stereotaxic apparatus. When necessary, supplementary doses of urethane (0.3 g/kg, i.p.) or pentobarbital (20 mg/kg, i.p.) were applied to maintain the rats at a constant level of anesthesia through the experiments. Rectal temperature was maintained at 36–37°C using a thermostat-controlled radiation heater. The skull and the dura over the left somatosensory cortex were removed. The exposed brains were covered with warm mineral oil to prevent them from drying out.

A monopolar tungsten electrode coated with glass except for the tip (approximately 150 μm in length and 50 μm in diameter) was placed in the left medial lemniscus (ML) (coordinates: A = −6.3, L = 1.0, H = −8.5 from Bregma, according to the atlas by Paxinos and Watson [34]). Current pulses (0.13–0.35 mA in amplitude, 0.1 ms in duration and 50–500 ms in interpulse interval) were delivered from an isolated stimulator (SEN-7103 and SS-302J, Nihon Kohden Co., Tokyo) to ML through the monopolar tungsten electrode. The site of the stimulation was histologically verified by a small lesion made by passing a negative DC current (50 μA, 30 s) through the monopolar electrode at the end of the experiments.

Field potential recording from the cortical surface was performed with a silver ball electrode or a glass-coated tungsten electrode. The reference electrode was a 5 × 10 mm silver plate which was inserted between the temporal

muscle and the skull. Field potential responses to a periodic ML fiber stimulation were detected by a conventional AC amplifier with a band-pass filter (1.5–3k Hz, 12 dB/oct). Field potential responses and current pulses were stored in a PCM data recorder (PCM processor: PCM-501ES, Sony Co., Tokyo, and video cassette recorder: A-88HF, Toshiba Co., Tokyo) for later analyses.

2.2. Data analyses

Field potential responses stored in the PCM data recorder were reproduced through a low-pass filter (50 Hz, 24 dB/oct; E-3201A, NF Co., Tokyo), as shown in Fig. 1a (upper trace). The second and the third traces in Fig. 1a are time derivatives of the smoothed field potential responses and current pulses for ML stimulation respectively. The field potential responses V and their time derivatives dV/dt were digitized by an A/D converter (DAS-1298BPC-16, Micro Science Co., Tokyo), and analyzed by a personal computer (PC9801-RX, NEC Co., Tokyo). The trajectory of the thirteen responses in Fig. 1a is shown in Fig. 1b. In later figures, the responses to dozens or hundreds current pulses were used to reconstruct attractors in the phase space (V, dV/dt). In the case of periodic responses, the attractor is a closed curve. However, a chaotic trajectory fills up a limited phase space due to instability and nonlinearity. Consequently, a strange attractor is reconstructed. Reconstruction of attractors is useful in visualizing chaos. However, many of the spreading attractors due to random noise are seemingly not distinguishable from strange attractors. In other words, only to look at spreading attractors of irregular responses is not sufficient to judge whether the responses are chaotic or random. Geometrical characteristics of strange attractors such as stretching and folding process should be investigated.

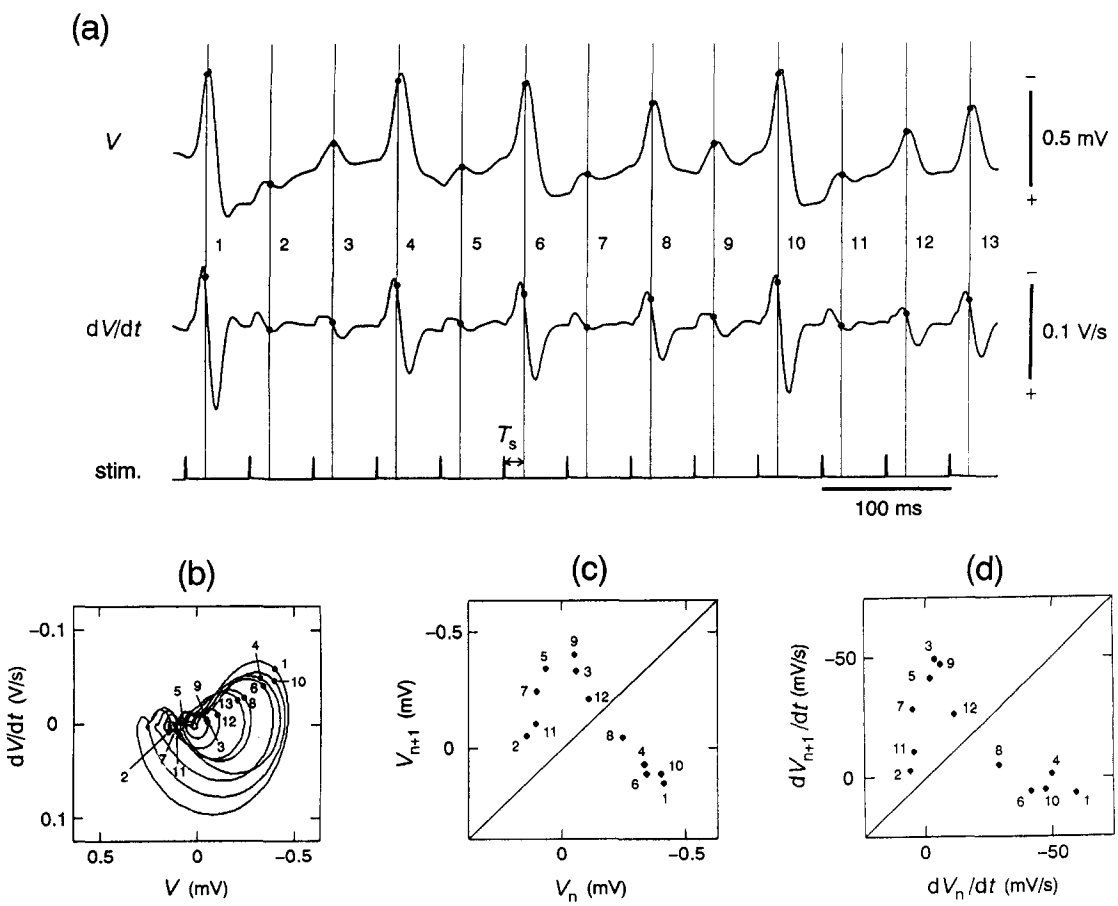

Fig. 1. Analyses of the experimental data. Field potential responses of the somatosensory cortex and stimulus current pulses stored in a PCM data recorder were reproduced and analyzed by a personal computer. The amplitude of field potential responses reflects the number of active neurons and the degree of synchronization. (a) The upper trace is smoothed field potential responses $V(t)$ obtained through a low-pass filter (50 Hz, 24 dB/oct). The middle trace is time derivatives of field potential responses dV/dt obtained through a circuit for differentiation. The lower trace is current pulses for ML fiber stimulation. The field potential responses and their time derivatives were sampled at T_S after each stimulus current pulse. (b) The trajectory in the two-dimensional phase space (V, dV/dt). The points numbered from 1 to 13 in the phase space correspond to the stroboscopically sampled points in a, and the points form a Poincaré cross-section. (c,d) One-dimensional strobomaps obtained from the sampled points; the sampled points were successively plotted against the preceding one. Numbered points on the maps correspond to the sampled points in a. If a one-dimensional map is a noninvertible function with unstable fixed points, irregular responses are chaotic.

Time series, V and dV/dt, were sampled at T_S after each stimulus current pulse, and a sequential series, (V_1, dV_1/dt), (V_2, dV_2/dt), (V_3, dV_3/dt),..., was obtained, as shown in Fig. 1a. Such stroboscopically sampled points form a Poincare cross-section of the attractor, as shown in Fig. 1b. Stretching and folding process of the strange attractor was observed as T_S-dependence of the cross-section. One-dimensional strobomaps $V_n \rightarrow V_{n+1}$ in Fig. 1c and $dV_n/dt \rightarrow dV_{n+1}/dt$ in Fig. 1d were also obtained from the sequential series (V_1, V_2,...) and (dV_1/dt, dV_2/dt,...) respectively. Numbers of the sampled points in Fig. 1b–d correspond to numbers of the points in Fig. 1a. If a map reconstructed by many sampled points is a noninvertible function with unstable fixed points, the irregular motion of the sampled points is subject to a deterministic law and chaotic. In contrast to the chaotic oscillations, maps of random oscillations never show any function. In the case of periodic oscillations with period m, the one-dimensional strobomap shows only m points.

In addition to the above analyses, power spectra of the responses were obtained. Moreover, correlation dimensions and the largest Lyapunov exponents of the responses were calculated using the Grassberger and Procaccia's algorithm [15] and Wolf's algorithm [52], respectively.

3. Results

3.1. Evoked potential and spontaneous EEG rhythm

Fig. 2a and b show field potentials of the somatosensory cortex recorded by an extracellular electrode on the cortical surface. A field potential response to a single current pulse for ML fiber stimulation is composed of a positive potential with a short latency and a subsequent, large negative potential, as shown in Fig. 2a. The amplitude of the negative potential increases with an increase in the current pulse, and the negative potential fluctuates when ML fibers are repetitively stimulated by current pulses. Therefore, the negative potentials were focused in the analyses. The origin of the negative potential on the cortical surface is polysynaptic activities of superficial layers organized horizontally in the somatosensory cortex [30,39].

Field potential responses that reflect the cortical activity depend on the depth of anesthesia. Therefore, two criteria were introduced to control the cortical activity in the experiments. One criterion is that spindle oscillations ($\approx$ 10 Hz) occur after the fast response to a single shock to ML fibers, as shown in Fig. 2b. The other criterion is that the

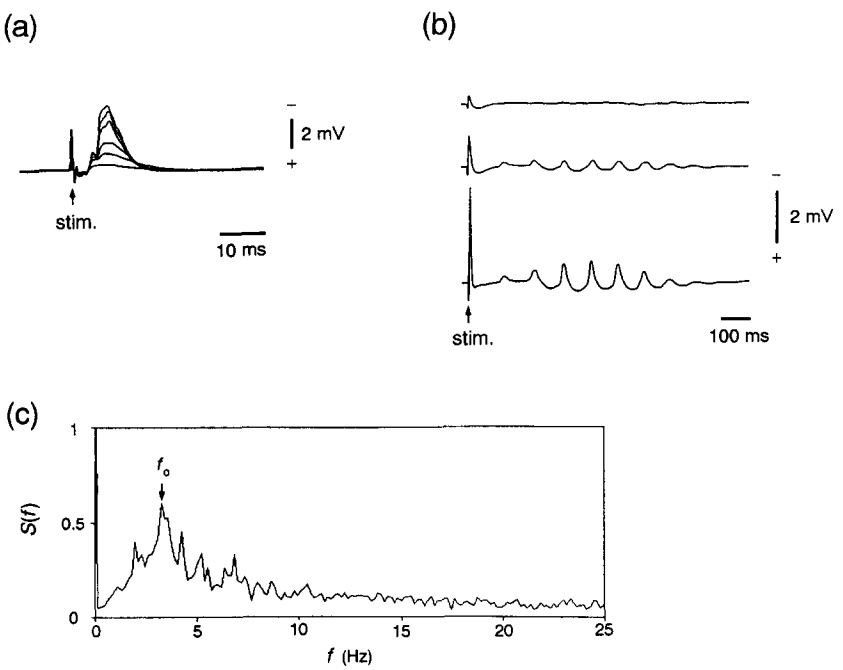

Fig. 2. Field potential responses of the somatosensory cortex to a single ML fiber stimulation and the power spectrum of spontaneous field potential oscillations. (a) Each field potential response was averaged 20 times. The amplitude of the negative component of the response increases with an increase in the ML fiber stimulation. The intensity of each current pulse for ML stimulation was 0.11, 0.13, 0.15, 0.2, 0.25, 0.3 mA. (b) Each trace is the field potential response averaged 20 times. Spindle oscillations are caused after the response shown in a. The frequency of the spindle oscillations is about 10 Hz. The amplitude of the oscillations increases with an increase in the ML fiber stimulation. The intensity of each current pulse for ML stimulation was 0.11, 0.15, 0.25 mA. (c) Power spectrum of spontaneous field potential oscillations without ML stimulation. The power spectrum was averaged 5 times using a time series for 30 s. The arrow indicates the dominant frequency of the spontaneous oscillations; $f_o = 3.3$ Hz. Dominant frequencies were distributed from experiment to experiment, and the average of the frequencies was 3.30 Hz ($n = 71$).

dominant frequency of the spontaneous field potential rhythm (f_o) is in the frequency range of the delta wave, as shown in Fig. 2c. The average of the frequencies was 3.30 Hz ($n = 71$).

3.2. Drift of the field potential responses to a long-lasting periodic ML stimulation

The pattern of field potential responses varies during a long-lasting periodic ML fiber stimulation, as shown in Fig. 3. The frequency of the stimulation f_i is 7.8 Hz. Although the responses are inhibited immediately after the beginning of the stimulation, stable negative augmented responses are caused after about the fiftieth stimulus pulse. The field potential responses are irregular between the 50th and the 300th current pulses. One large response occurs every two current pulses between the 300th and the 550th pulses (1:2 phase-locking). 1:1 phase-locking occurs after the 560th pulse though the amplitude of the responses fluctuates.

In Fig. 3 the dominant frequency of spontaneous field potential oscillations f_o is 2.8 Hz (delta wave) before the ML fiber stimulation is applied. However, the dominant frequency f_o is 8.6 Hz (alpha wave) after the stimulation is removed. This suggests that the frequency of the spontaneous field potential rhythm which reflects the cortical state is changed by the repetitive ML fiber stimulation. Therefore, although there is no direct evidence, it is plausible that 1:1 phase-locked responses to the later part of the long-lasting ML fiber stimulation are caused by the interaction between the cortical 8.6 Hz rhythm and the 7.8 Hz ML stimulation; the ratio f_i/f_o is about 1.

The following procedures were taken when field potential responses were quantitatively analyzed. The number of current pulses delivered to ML fibers was limited to 300 in order to hold the cortical state within a small drift. Power spectra of spontaneous cortical oscillations were calculated using time series for 20 s before ML stimulation was applied, and the frequency f_o was obtained. The frequency of ML stimulation f_i was normalized by f_o. The amplitude of stimulus current pulses I was also normalized by the threshold current I_{th} that initiated a negative field potential. The normalized stimulus intensity I/I_{th} and the normalized frequency f_i/f_o were used as stimulus parameters.

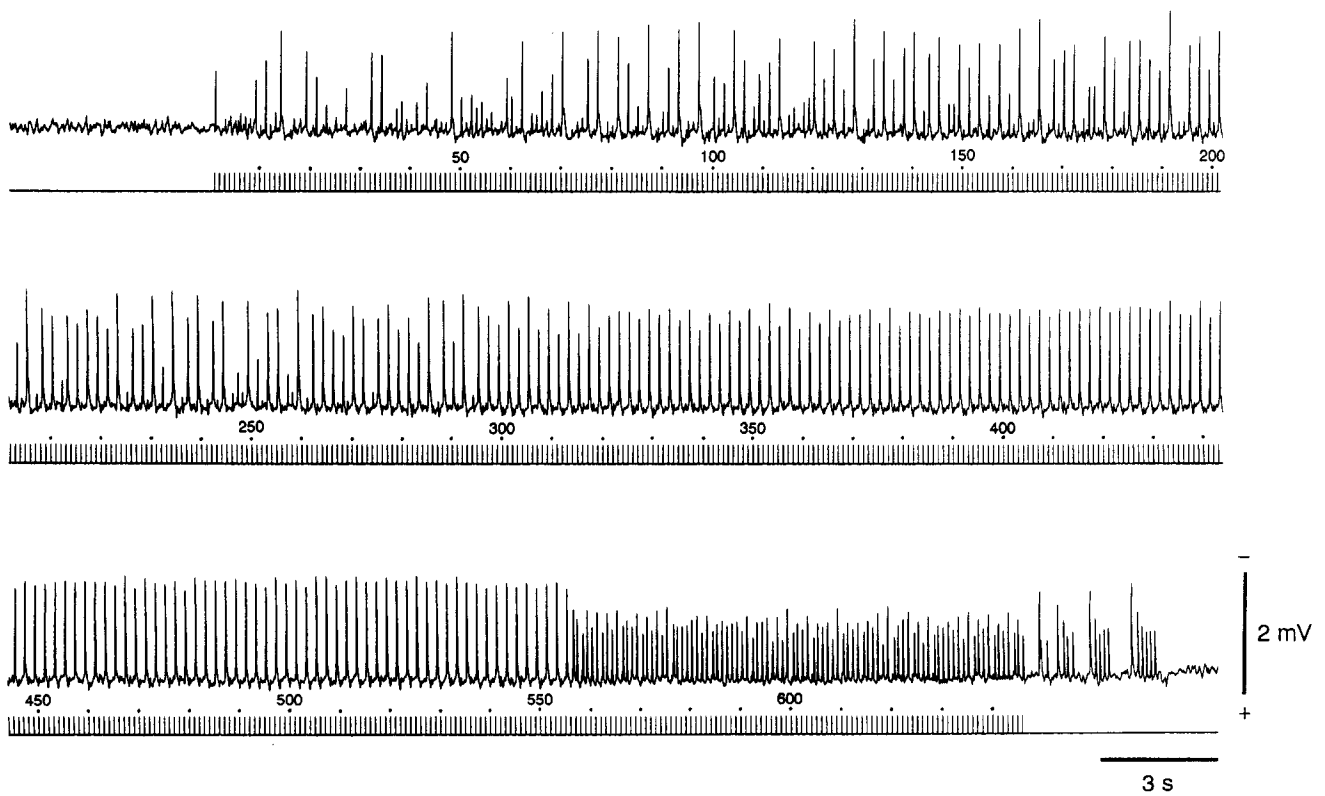

Fig. 3. Time series of field potential responses of the somatosensory cortex caused by a long-lasting, periodic ML fiber stimulation. Field potential responses were observed under pentobarbital anesthesia. The upper and the lower traces in each panel are field potential responses and stimulus current pulses, respectively. Current pulses are numbered. The frequency of ML stimulation is 7.8 Hz. The amplitude and the duration of current pulses are 0.2 mA and 0.1 ms, respectively. Although the responses are inhibited immediately after applying the stimulation, stable negative responses are caused after about the 50th current pulse. The response pattern varies with time; irregular responses → 1:2 phase locking (between the 300th and the 550th pulses) → 1:1 phase-locking (after the 560th pulse). The delta activity (2.8 Hz) is dominant in the spontaneous field potential oscillations before the ML fiber stimulation is applied. However, the alpha activity (8.6 Hz) is dominant after the stimulation is removed. The cortical state is changed by the long-lasting ML fiber stimulation.

3.3. Phase-locked responses

The upper panels in Fig. 4 show n:m (n = 1,2; m = 1,2,3) phase-lockings, that is n field potential responses occur every m current pulses for ML fiber stimulation. When I/I_{th} = 1.87 and f_i/f_o = 1.43, field potential responses are well synchronized with current pulses, as shown in Fig. 4a. As small field potential responses exist in Fig. 4b and c, the criterion of field potential response, i.e., synchronized response of a neural assembly, was set; the amplitude of field potential responses must be more than 30% of that of the largest response. For instance, small negative potentials in Fig. 4b were judged to be field potential responses, because the amplitude of the small responses are about 35% of the largest response. Therefore, large and small responses are caused by turns by a periodic ML stimulation, namely 2:2 phase-locking. It was judged that small negative potentials in Fig. 4c were not field potential responses, because the amplitude of the small negative potentials are about 23% of the largest one. Therefore, the responses were classified as 1:2 phase-locking. Fig. 4d shows 1:3 phase-locking.

The middle panels in Fig. 4 show attractors reconstructed in the two-dimensional phase space (V, dV/dt). The attractors are closed curves reflecting the phase-lockings, although the attractors are bundles of trajectories due to random noise. The lower panels in Fig. 4 show one-dimensional strobomaps obtained from sequential series of field potential sampled every period of ML fiber stimulation. The strobomap of the 1:1 phase-locking in Fig. 4a shows that sampled field potentials cluster around a stable fixed point on the diagonal line. The maps of the 2:2 and the 1:2 phase-lockings in Fig. 4b and c show two symmetric clusters for the diagonal line. The sampled field potentials are alternately mapped on the two clusters. The strobomap of the 1:3 phase-locking in Fig. 4d shows three clusters, that is the sampled potentials are successively mapped on the clusters. A spread of the clusters would be due to random noise.

3.4. Chaotic responses

Irregular field potential responses caused by a periodic ML fiber stimulation were classified into four kinds of

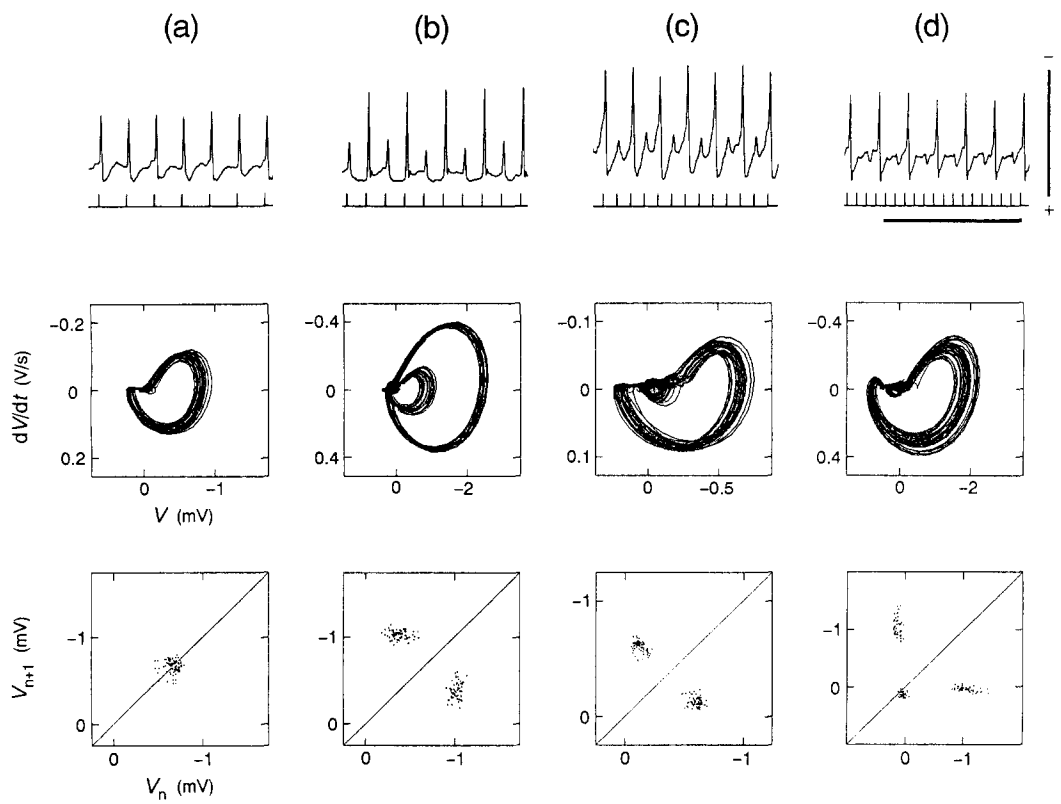

Fig. 4. Phase-locked responses of the somatosensory cortex caused by a periodic ML fiber stimulation. The upper panels are time series of field potential responses. The middle and the lower panels are two-dimensional attractors and one-dimensional strobomaps, respectively. Initial transients of the responses for 50–100 periods of the stimulation were discarded. (a) 1:1 phase-locking. I/I_{th} = 1.87. f_i/f_o = 1.43. The attractor was reconstructed from a time series for 6 s (30 current pulses). The number of sampled points in the one-dimensional map is 96. T_S = 14 ms. (b) 2:2 phase-locking. I/I_{th} and f_i/f_o are 3.18 and 1.93, respectively. The attractor was reconstructed from a time series for 7 s (50 current pulses). The number of sampled points in the one-dimensional map is 131. T_S = 14 ms. (c) 1:2 phase-locking. I/I_{th} and f_i/f_o are 1.87 and 2.86, respectively. The attractor was reconstructed from a time series for 6.2 s (62 current pulses). The number of sampled points in the one-dimensional map is 150. T_S = 14 ms. (d) 1:3 phase-locking. I/I_{th} and f_i/f_o are 1.8 and 5.29, respectively. The attractor was reconstructed from a time series for 8.9 s (127 current pulses). The number of sampled points in the one-dimensional map is 131. T_S = 14 ms. The vertical bar indicates 2 mV for a, 4 mV for b and d and 1 mV for c. The horizontal bar indicates 1 s.

chaotic responses. Fig. 5a shows chaotic responses caused in the parameter region between the 1:1 and the 2:2 phase-lockings. These chaotic responses appear to be a mixture of 1:1 and 2:2 phase-lockings. Small spindle waves also occur on occasion as the stimulation is relatively strong. Chaotic responses caused in the transition region between the 1:1 and the 1:2 phase-lockings are shown in Fig. 5b. These chaotic responses are a mixture of 1:1 and 1:2 phase-lockings. Chaotic responses in Fig. 5c are a mixture of 1:2 and 1:3 phase-lockings caused in the transition region between the 1:2 and the 1:3 phase-lockings. Fig. 5d shows chaotic responses caused by a relatively high frequency stimulation. These chaotic responses do not appear to be a simple mixture of two kinds of phase-lockings.

Power spectra of the four kinds of chaotic responses in Fig. 5 are shown in Fig. 6. The power spectrum in Fig. 6a obtained from the responses in Fig. 5a consists of frequency components of f_i and $f_i/2$ and their harmonics. f_i

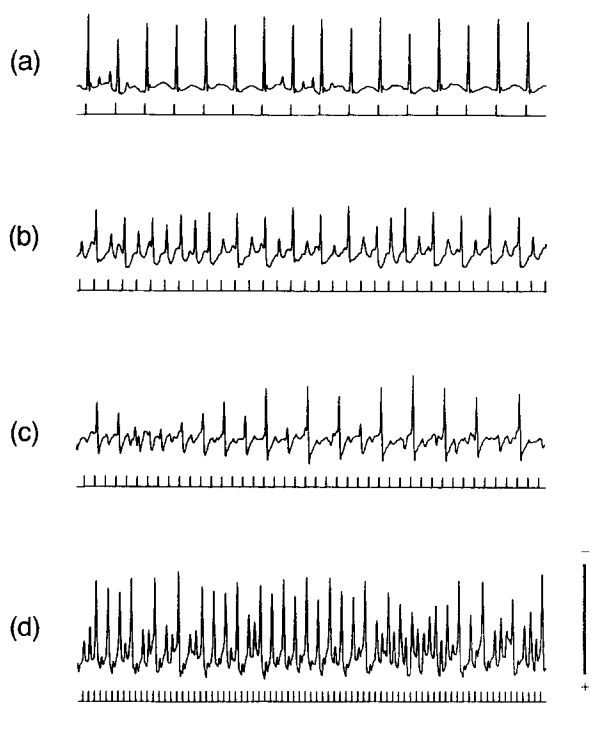

Fig. 5. Time series of chaotic field potential responses of the somatosensory cortex caused by a periodic ML fiber stimulation. The upper and the lower traces in each panel are 4 s segments of field potential responses and stimulus current pulses, respectively. (a) Chaotic responses caused in the transition region between the 1:1 and the 2:2 phase-lockings. Small spindle waves occasionally occur as the stimulation is relatively strong. I/I_{th} and f_i/f_o are 3.18 and 1.08, respectively. (b) Chaotic responses in the transition region between the 1:1 and the 1:2 phase-lockings. I/I_{th} and f_i/f_o are 2.27 and 2.51, respectively. (c) Chaotic responses in the transition region between the 1:2 and the 1:3 phase-lockings. I/I_{th} and f_i/f_o are 1.8 and 4.58, respectively. (d) Chaotic responses. These responses do not appear to be a mixture of two kinds of phase-lockings. I/I_{th} and f_i/f_o are 2.27 and 5.12, respectively. The vertical bar is 4 mV for a and c, 2 mV for b and 1 mV for d. The horizontal bar is 1 s.

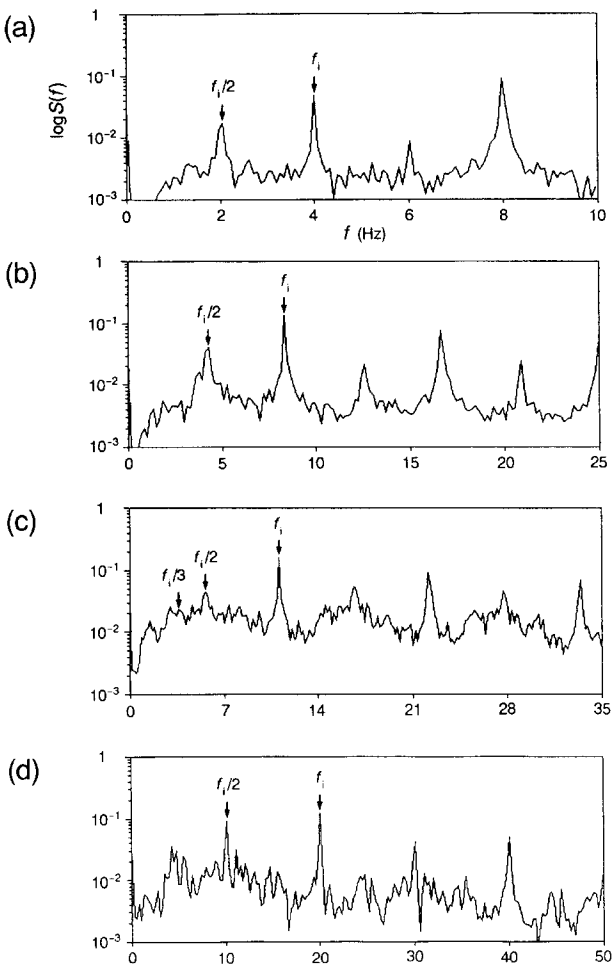

Fig. 6. Power spectra of chaotic field potential responses of the somatosensory cortex caused by a periodic ML fiber stimulation. Power spectra in a–d were obtained from the chaotic responses shown in Fig. 5a–d, respectively. Each power spectrum was averaged 2–5 times using a time series for 8–49 s. Initial transients of the responses for 50–100 current pulses were discarded. f_i is the frequency of ML fiber stimulation. (a) The power spectrum has peaks at f_i, $f_i/2$ and their harmonics and is consistent with a mixture of 1:1 and 2:2 phase-lockings. The largest spectral peak at $2f_i$ corresponds to the second harmonic oscillations and the spindle waves which occur on occasion. $f_i = 4$ Hz. (b) The power spectrum also has peaks at f_i, $f_i/2$ and their harmonics, because these chaotic responses are a mixture of 1:1 and 1:2 phase-lockings. $f_i = 8.3$ Hz. (c) Spectral peaks at f_i, $f_i/2$, $f_i/3$ and their harmonics exist. The power spectrum is consistent with a mixture of 1:2 and 1:3 phase-lockings. The broad band spectrum indicates that the responses are quite irregular. $f_i = 11.1$ Hz. (d) Besides the spectral peaks at f_i, $f_i/2$ and $f_i/4$, various peaks exist in the power spectrum. $f_i = 20$ Hz.

is the frequency of periodic ML fiber stimulation. Therefore, the spectrum indicates that the chaotic responses are a mixture of 1:1 and 2:2 phase-lockings. The largest component of $2f_i$ corresponds to the second harmonic oscillations and the spindle waves which occur on occasion. The power spectrum in Fig. 6b obtained from the responses in Fig. 5b is similar to the spectrum in Fig. 6a, because the chaotic responses are a mixture of 1:1 and 1:2 phase-lockings. Fig. 6c shows the power spectrum of the responses in

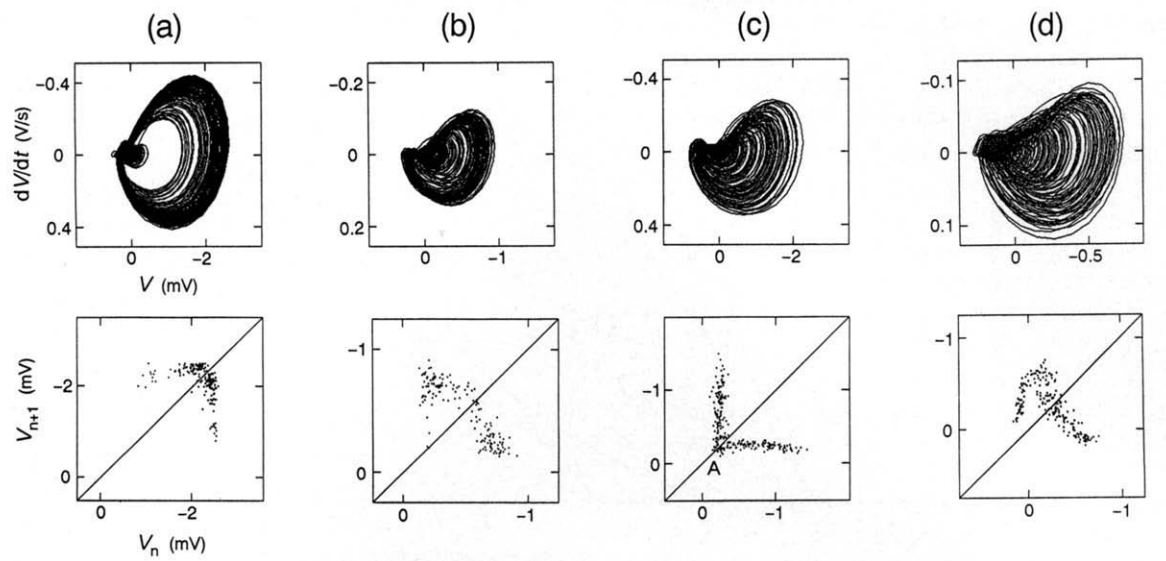

Fig. 7. Two-dimensional attractors and one-dimensional strobomaps of chaotic field potential responses of the somatosensory cortex to a periodic ML fiber stimulation. The upper panels are two-dimensional attractors, and the lower panels are one-dimensional strobomaps. Attractors and one-dimensional maps in a–d were obtained from the field potential responses in Fig. 5a–d, respectively. Initial transients of the responses for 50–100 current pulses were discarded. (a) Chaotic responses observed in the transition region between the 1:1 and the 2:2 phase-lockings. The attractor was reconstructed from a time series for 49.5 s (198 current pulses). The number of sampled points on the strobomap is 200. $T_S = 14$ ms. (b) Chaotic responses observed in the transition region between the 1:1 and the 1:2 phase-lockings. The attractor was reconstructed from a time series for 22 s (183 current pulses). The number of sampled points on the strobomap is 158. $T_S = 14$ ms. (c) Chaotic responses observed in the transition region between the 1:1 and the 1:3 phase-lockings. The attractor was reconstructed from a time series for 22 s (244 current pulses). The number of sampled points on the strobomap is 250. $T_S = 18$ ms. (d) Chaotic responses. The attractor was reconstructed from a time series for 7 s (140 current pulses). The number of sampled points on the strobomap is 200. $T_S = 14$ ms. Although these attractors are seemingly not distinguishable, the strobomaps are obviously different. All of the maps are noninvertible functions. The slope of the maps in a, b and d at the fixed points is more negative than -1. This indicates that these responses are chaotic. The map in c is probably discrete and consists of two branches. This irregular motion of the trajectory is an intermittent chaos.

Fig. 5c. Spectral peaks at f_i and $f_i/2$ and their harmonics exist, and frequency components of $f_i/3$ and its harmonics can also be seen. Therefore, the power spectrum is consistent with a mixture of 1:2 and 1:3 phase-lockings. Moreover, the broad band spectrum well characterizes the irregularity of the responses. Besides the spectral peaks at f_i and $f_i/2$, various peaks exist in the power spectrum in Fig. 6d. The chaotic responses shown in Fig. 5d are characterized by the broad band spectrum with these peaks.

Attractors shown in Fig. 7a–d (upper panels) were reconstructed in the phase space (V, dV/dt) from the chaotic responses shown in Fig. 5a–d, respectively. All the attractors were widely spread, and the attractors in Fig. 7b–d are seemingly not distinguishable.

One-dimensional strobomaps of the chaotic field potential responses in Fig. 5a–d are shown in Fig. 7a–d (lower panels), respectively. Each strobomap reveals a noninvertible function, though the map has a certain thickness due to random noise. Fixed points of the maps in Fig. 7a, b and d, i.e., the intersections between the functions and the diagonal line, are unstable, because the slopes of the maps at the fixed points are more negative than -1. This indicates that the irregularity is subject to a deterministic law, and information about initial conditions is rapidly lost. Actually, the trajectory on the one-dimensional strobomap spirals away from the unstable fixed point. However, the trajectory returns to somewhere near the fixed point after several iterations, because the map is nonlinear and has a single hump. Then, the trajectory spirals away again. Since the trajectory cannot stay at the unstable fixed point, it wanders from place to place on the map. The noninvertibility of the map with an unstable fixed point is undoubted evidence for the chaotic responses of the somatosensory cortex to a periodic ML fiber stimulation in vivo. The one-dimensional strobomap in Fig. 7c

Table 1
Largest Lyapunov exponents and correlation dimensions of the spontaneous and the evoked field potential oscillations

Type	Largest Lyapunov exponent (s^{-1})	Correlation dimension
Spontaneous (delta rhythm)	3.4 ± 1.2 (8)	5.5 ± 0.4 (8)
Phase-lockings	4.4 ± 1.0 (14)	1.5 ± 0.3 (5)
Chaotic responses (between phase-lockings)	7.3 ± 2.1 (9)	*
Chaos	12.6 ± 2.9 (9)	2.8 ± 0.2 (7)

Results are expressed in mean ± standard deviation. Numbers in parentheses indicate the number of events. The symbol * indicates that the slope of correlation functions does not saturate, even if the embedding dimension increases up to 20 because of the noise superposed on the responses.

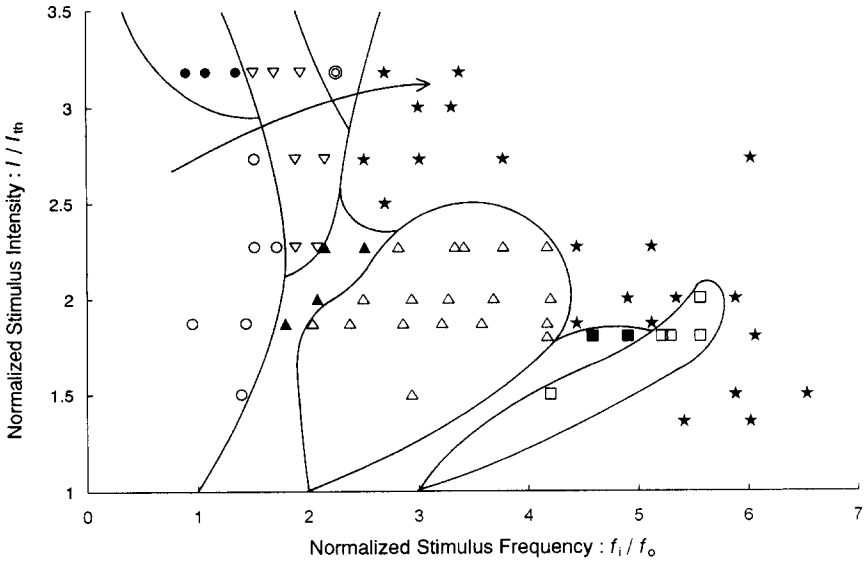

Fig. 8. Phase diagram of field potential responses of the somatosensory cortex to a periodic ML fiber stimulation. Abscissa is the normalized stimulus frequency f_i/f_o and ordinate is the normalized stimulus intensity I/I_{th}. In the regions with open symbols, ○, ▽, ⊙, △, □, 1:1, 2:2, 2:4, 1:2 and 1:3 phase-lockings occur, respectively. In the transition regions with closed symbols, ●, ▲, ■, adjacent phase-lockings are mixed, and the responses are chaotic. In the region with closed stars (★), the chaotic responses shown in Fig. 5d occur. The curve with an arrowhead indicates a route from the 1:1 phase-locking to the chaos through a cascade of period-doubling bifurcations.

is probably discrete and consists of two branches. The trajectory approaches the diagonal line along the lower branch and moves slowly near the point A. Then, the trajectory rapidly escapes from the diagonal line along the upper branch and jumps to the lower branch. This irregular motion of the trajectory is a typical example of intermittent chaos [4,19].

3.5. Correlation dimension and the largest Lyapunov exponent

The correlation dimensions and the largest Lyapunov exponents of the field potential responses in the somatosensory cortex are shown in Table 1. The low noninteger correlation dimensions and the positive Lyapunov

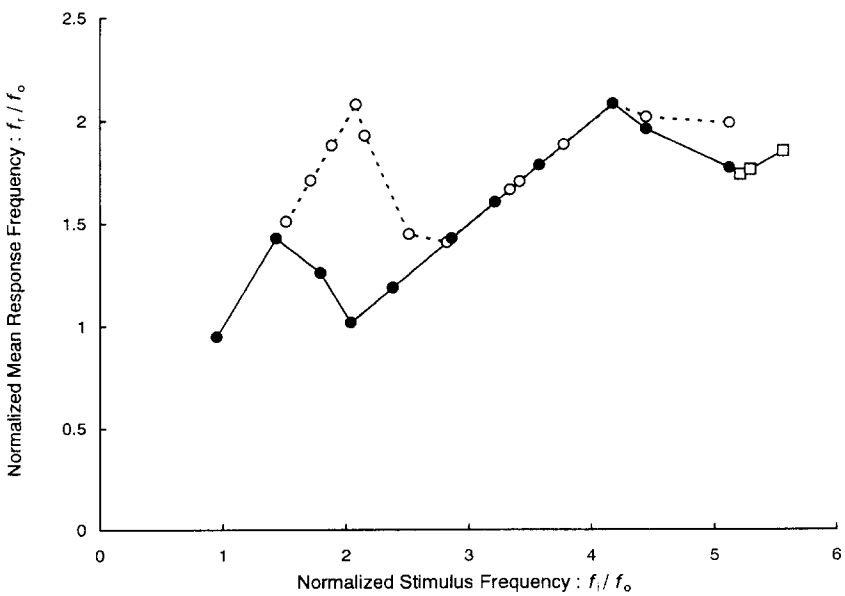

Fig. 9. Mean response frequency of field potential in the somatosensory cortex to a periodic ML stimulation. Abscissa and ordinate are the normalized stimulus frequency f_i/f_o and the mean response frequency f_r/f_o, respectively. The straight-line segments which coincide with the lines, $f_r = f_i/n$ (n = 1, 2, 3), indicate that 1:n phase-lockings occur. The line segment in the f_i/f_o range below 2.08 at I/I_{th} = 2.27 also corresponds to 2:2 phase-lockings. The normalized mean response frequency abruptly changes in the transition regions between phase-locking states. Chaotic responses occur in the transition regions. Closed circles: I/I_{th} = 1.87; open squares: I/I_{th} = 1.8; open circles: I/I_{th} = 2.27.

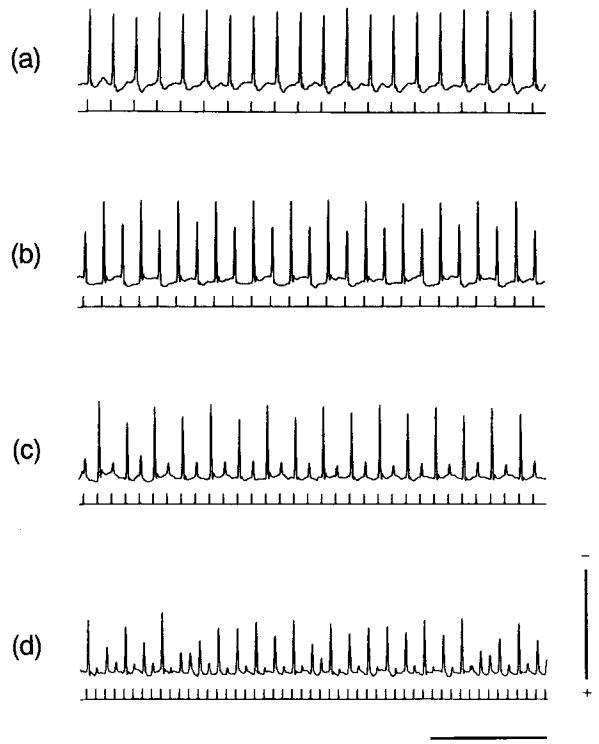

Fig. 10. Period-doubling bifurcations of field potential responses of the somatosensory cortex to a periodic ML fiber stimulation. Examples of time series of field potential responses observed along the curve with an arrowhead in Fig. 8 are given. The upper and the lower traces in each panel are field potential responses and stimulus current pulses, respectively. (a) 1:1 phase-locking. I/I_{th} and f_i/f_o are 2.73 and 1.51, respectively. (b) 2:2 phase-locking. I/I_{th} and f_i/f_o are 3.18 and 1.69, respectively. Large and small responses are caused by turns. (c) 2:4 phase-locking. One large, one middle and two small responses occur every four current pulses. I/I_{th} and f_i/f_o are 3.18 and 2.25, respectively. (d) Chaotic response. I/I_{th} and f_i/f_o are 3.18 and 3.37, respectively. The vertical bar indicates 2 mV for a and 4 mV for b, c and d. The horizontal bar indicates 1 s.

exponents of the chaotic responses are consistent with the evidence provided in the previous section. However, the estimation of these values is quite sensitive to random noise contamination. Actually, random noises are superposed on the field potential responses observed in the experiments. Probably, besides random noise generated in the experimental apparatus, some other random noise is intrinsically generated in cortical neural networks; the size of synchronized neural assemblies would fluctuate, and neuronal activities in the assembly would not perfectly synchronize with each other. Therefore, the correlation dimensions of the phase-lockings are larger than unity, and the correlation dimensions of the chaotic responses would be overestimated. The largest Lyapunov exponents of the phase-lockings are also positive. In other words, positive Lyapunov exponents of field potential responses observed experimentally are not always evidence for chaotic activity of neural assemblies.

The correlation dimensions of the field potential responses to a ML fiber stimulation are lower than the correlation dimensions of the spontaneous field potential oscillations. The decrease in the correlation dimension appears to indicate an increase in the synchronization of neural activities in thalamo-cortical networks. The difference between the Lyapunov exponents of the phase-lockings and the chaotic responses is significant. Therefore, the largest Lyapunov exponent may be used as an indicator of relative difference in dynamical features of field potential responses.

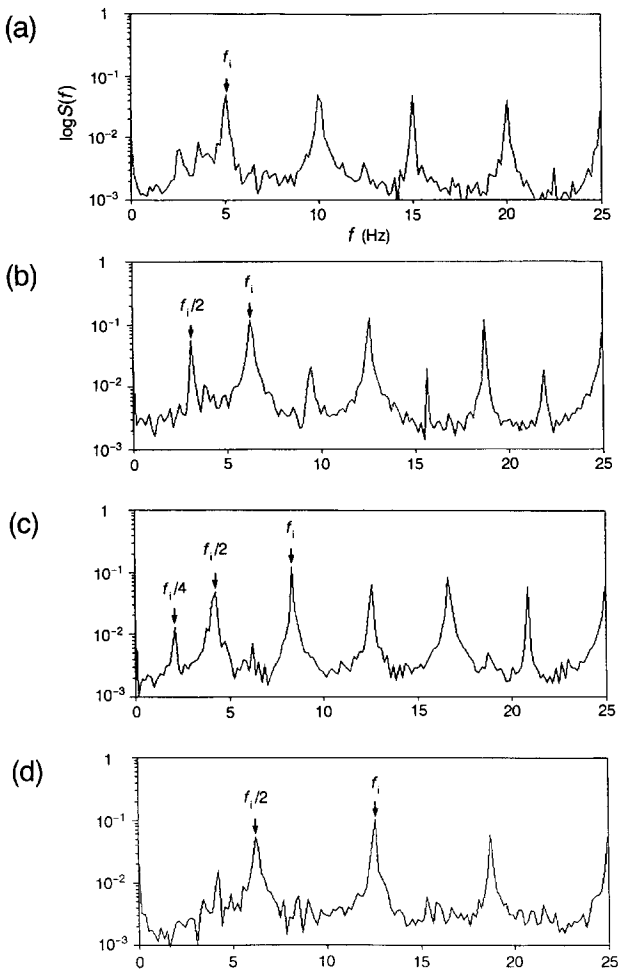

Fig. 11. Power spectra of field potential responses observed on a route to the chaos through a cascade of period-doubling bifurcations. Power spectra in a–d were obtained from the field potential responses shown in Fig. 10a–d. Initial transients of the responses for 20–100 current pulses were discarded. f_i is the frequency of ML fiber stimulation. (a) 1:1 phase-locking. $f_i = 5$ Hz. The power spectrum shows peaks at f_i and its harmonics. (b) 2:2 phase-locking. $f_i = 6.25$ Hz. The power spectrum shows peaks at f_i, $f_i/2$ and their harmonics. (c) 2:4 phase-locking. $f_i = 8.33$ Hz. The power spectrum shows peaks at f_i, $f_i/2$, $f_i/4$ and their harmonics. (d) Chaotic responses. $f_i = 12.5$ Hz. The power spectrum is not broadened but primarily shows peaks at f_i and $f_i/2$. The reason would be that relatively large responses are frequently caused every two periods of the stimulation, though responses of various amplitudes are included in the chaotic responses.

3.6. Phase diagram of field potential responses

A phase diagram of the field potential responses of the somatosensory cortex to a periodic ML fiber stimulation is shown in Fig. 8. Control parameters are the normalized intensity I/I_{th} and the normalized frequency f_i/f_o of current pulses used for periodic ML stimulation. Larger current pulses excite more ML fibers, so that more impulses are delivered to thalamo-cortical networks.

1:1, 2:2, 2:4, 1:2 and 1:3 phase-lockings occur in the regions with open symbols, ○, ▽, ⊙, △, □, respectively. In the transition regions with closed symbols, ●, ▲, ■, between the phase-lockings, chaotic responses occur. These chaotic responses are mixtures of two kinds of phase-lockings, as shown in Fig. 5a–c. In the region with closed stars (★), chaotic responses occur, but they are not simple mixtures of two kinds of phase-lockings. Each kind of the chaotic responses is characterized by a noninvertible one-dimensional strobomap, as shown in Fig. 7. A cascade of period doubling bifurcations was observed along the curve with an arrowhead. The details of the period doubling bifurcations will be given in Section 3.8.

3.7. Response frequency of the field potential

Fig. 9 shows the mean response frequency f_r of field potential responses of the somatosensory cortex as a function of the frequency f_i of periodic ML fiber stimulation. Both frequencies are normalized by the frequency f_o of the spontaneous cortical rhythm. The normalized mean response frequency f_r/f_o is proportional to the normalized stimulus frequency f_i/f_o in the frequency range below 2.08 when the stimulus intensity I/I_{th} is 2.27 (open circles connected by dotted lines). This is consistent with the 1:1 and the 2:2 phase-lockings. The straight-line segments of the solid curve in the ranges of f_i/f_o, 0.95–1.43, 2.04–4.17 and 5.21–5.56, coincide with the lines, $f_r = f_i$, $f_r = f_i/2$ and $f_r = f_i/3$, respectively. These indicate 1:1, 1:2 and 1:3 phase-lockings. The mean response frequency abruptly changes in the transition regions from one phase-locking state to another, that is f_r/f_o decreases with an increase in f_i/f_o. Chaotic responses occur in the transition regions.

3.8. Period-doubling bifurcations

When the frequency of ML fiber stimulation is increased along the curve with an arrowhead shown in Fig. 8, 1:1 phase-locking (period 1) successively bifurcates to 2:2 (period 2) and 2:4 (period 4) phase-lockings, and finally chaotic responses occur. Examples of these responses are shown in Fig. 10. In Fig. 10a, large field potential responses occur every period of the stimulation, namely 1:1 phase-locking. In the case of 2:2 phase-lock-

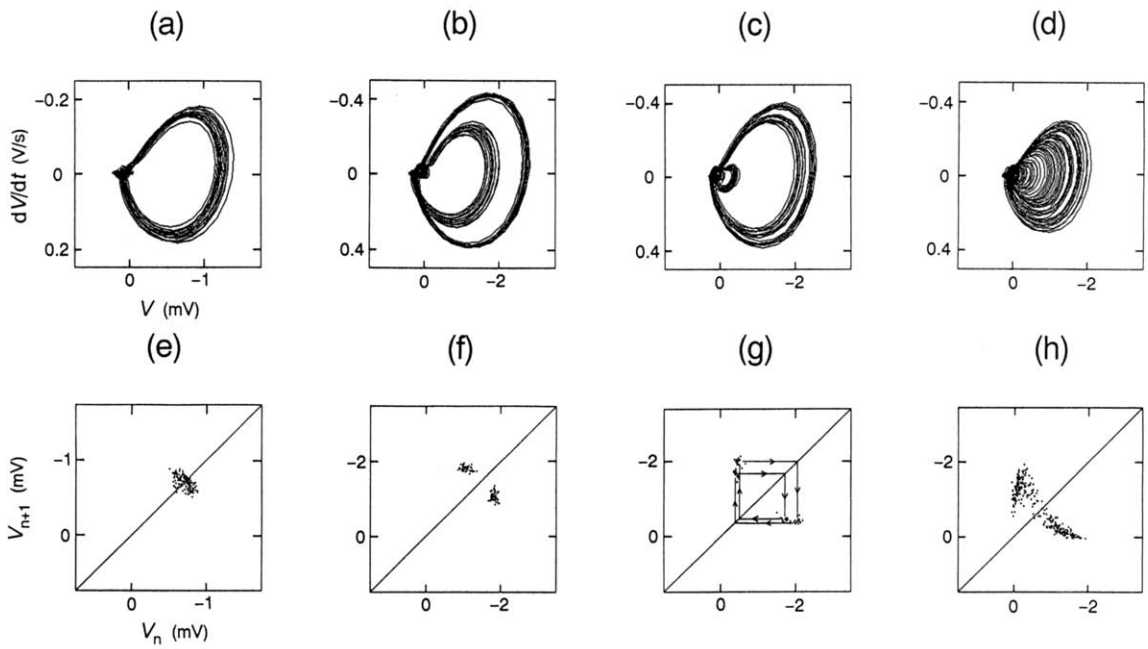

Fig. 12. Attractors and one-dimensional strobomaps of field potential responses observed on a route to the chaos through a cascade of period-doubling bifurcations. Attractors in a–d and strobomaps in e–h were obtained from the responses in Fig. 10a–d, respectively. Initial transients of the responses for 20–100 current pulses were discarded. (a) 1:1 phase-locking. The attractor was reconstructed from a time series for 5 s (25 current pulses). (b) 2:2 phase-locking. The attractor was reconstructed from a time series for 6 s (37 current pulses). (c) 2:4 phase-locking. The attractor was reconstructed from a time series for 6 s (50 current pulses). Attractors in a–c consist of one, two and four loops, respectively, though each loop expands to some extent. (d) Chaotic responses. The strange attractor was reconstructed from a time series for 8 s (100 current pulses). (e) 1:1 phase-locking. The number of sampled points on the strobomap is 150. T_S = 14 ms. Sampled field potentials cluster around a point on the diagonal line. (f) 2:2 phase-locking. The number of sampled points on the strobomap is 100. T_S = 14 ms. The map shows two clusters. (g) 2:4 phase-locking. The number of sampled points on the strobomap is 56. T_S = 14 ms. The map shows four clusters. The trajectory on the map visits four clusters in turn. (h) Chaotic responses. The number of sampled points on the strobomap is 280. T_S = 14 ms. The map shows a noninvertible function with an unstable fixed point which is similar to the map in Fig. 7d.

ing, large and middle responses alternately occur, as shown in Fig. 10b. In the case of 2:4 phase-locking (Fig. 10c), one large, one middle and two small responses occur every four periods of the stimulation. Responses of various sizes are contained in the chaotic responses in Fig. 10d.

Fig. 11 shows power spectra obtained from the responses shown in Fig. 10. f_i is the frequency of periodic ML fiber stimulation. These power spectra well demonstrate period-doubling bifurcations. The power spectrum in Fig. 11a shows that the 1:1 phase-locking has a single oscillatory mode of f_i. Besides the mode of f_i, the mode of $f_i/2$ emerges in the 2:2 phase-locking, and furthermore, the mode of $f_i/4$ emerges in the 2:4 phase-locking, as shown in Fig. 11b and c. The power spectrum of the chaotic responses in Fig. 11d primarily shows peaks at f_i and $f_i/2$. Although responses of various amplitudes are included in the chaotic responses, relatively large responses are frequently caused every two periods of the stimulation. This would be the reason why the spectrum is not broadened, yet two peaks are outstanding.

Fig. 12 shows attractors in the two-dimensional phase space reconstructed from the responses shown in Fig. 10. Attractors which correspond to the 1:1, the 2:2 and the 2:4 phase-lockings consist of one, two and four loops, respectively, though each loop is a bundle of trajectories (Fig. 12a, b and c). These attractors also demonstrate well the period-doubling bifurcations. The chaotic trajectory constructs a strange attractor as shown in Fig. 12d.

One-dimensional strobomaps of the responses in Fig. 10a–d are shown in Fig. 12e–h, respectively. Sequential

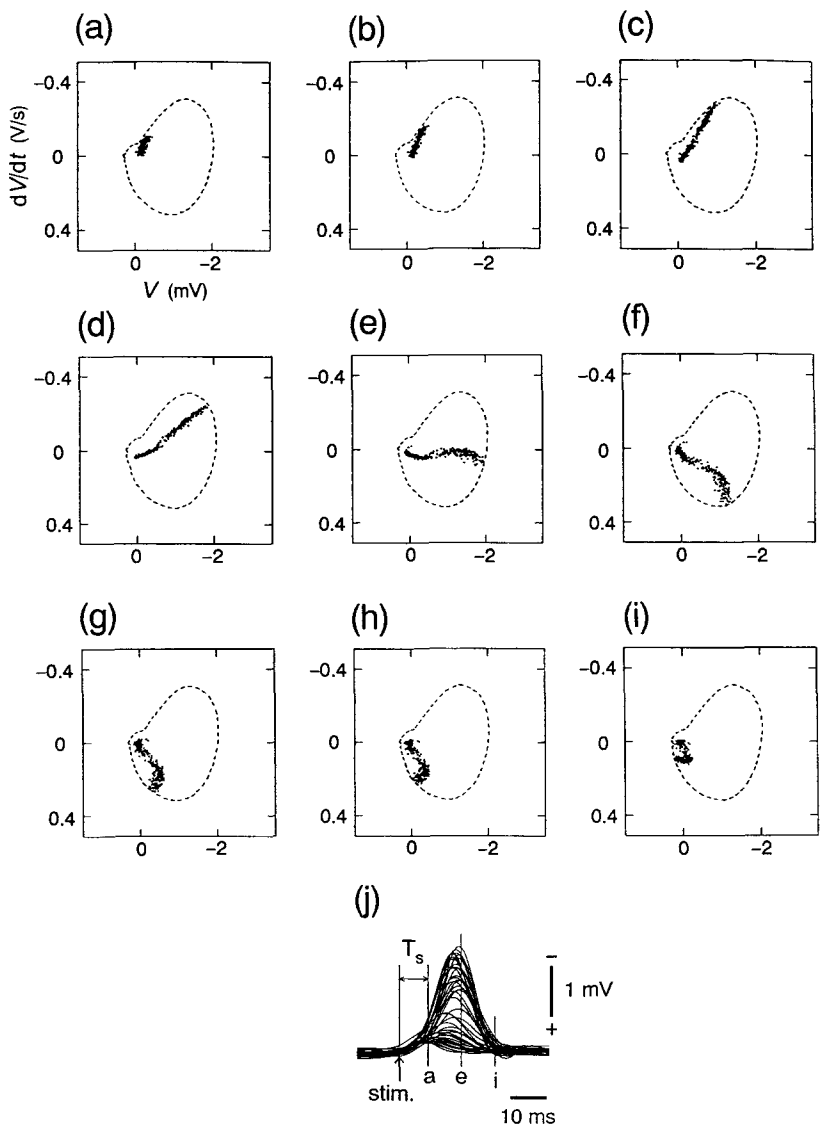

Fig. 13. Poincaré cross-sections of the attractor of chaotic responses. Stroboscopic cross-sections in a–i were obtained from the strange attractor shown in Fig. 12d. Dotted lines are the contour of the attractor. The cross-section is expanded (a–d) and then folded and contracted (e–i). T_S: a = 8, b = 9, c = 11, d = 14, e = 17, f = 20, g = 23, h = 24, i = 26 ms. (j) Fifty field potential responses to a ML fiber stimulation were superposed. Sampled points on each cross-section are mixed by stretching and folding process.

series of field potentials sampled 14 ms after each stimulus current pulse make a cluster around a stable fixed point on the diagonal line in Fig. 12e, two clusters in Fig. 12f and four clusters in Fig. 12g. These strobomaps well demonstrate that these phase-lockings are period one, period two and period four, respectively. For example, in the case of the 2:4 phase-locking, sampled field potentials are successively mapped on the four clusters, as shown in Fig. 12g. In the case of chaotic responses, the map reveals a noninvertible function with an unstable fixed point, as shown in Fig. 12h.

3.9. Stretching and folding process

Fig. 13 shows stroboscopic cross-sections of the strange attractor in Fig. 12d. T_S was varied from 8 to 26 ms, as shown in Fig. 13j. The cross-sections are line-shaped and depend on T_S. The cross-section is first expanded (Fig. 13a–d) and then folded and contracted (Fig. 13e–i). Therefore, sampled field potentials on each cross-section are mixed by the stretching and folding process, and the correlation between them rapidly decreases. In other words, the chaotic trajectory is mixed within a limited volume of the phase space. The stretching and folding process of the strange attractor is an essential mechanism for chaos generation [17,21].

4. Discussion

Spontaneous field potential rhythm in the somatosensory cortex was controlled by the depth of anesthesia to show delta waves around 3 Hz in the experiments. Neuronal activities would not well synchronize with each other in this state, because the amplitude of the spontaneous field potential rhythm is quite small. However, spindle oscillations around 10 Hz were evoked by a single shock to ML fibers. Stimulus-evoked spindle oscillations in the alpha range in cortico-thalamic structures have been studied [5,7,47], and it has been supposed that the spindle oscillations are evoked due to intrinsic, oscillatory properties of thalamic neurons [44]. Furthermore, it has been demonstrated that a model of the thalamocortical relay neuron causes various responses to rhythmic hyperpolarizations: for example, intermittent phase-lockings when the model spontaneously causes spindle oscillations [51]. Therefore, we expected that various nonlinear responses are caused by the interplay of spindle oscillations and a periodic ML fiber stimulation under the above conditions. However, spindle oscillations were immediately inhibited by a periodic ML fiber stimulation, and then field potential responses became chaotic. The field potential responses varied with time, and finally negative field potentials were synchronously caused by the periodic ML fiber stimulation. This paradoxical inhibition of spindle oscillations appears to reflect functional behavior of thalamo-cortical neurons: the gating function [28]. When spindle oscillations occur in the cortex, thalamic neurons are hyperpolarized and cause bursting discharges. Therefore, responsiveness of thalamic neurons to synaptic input is low, and sensory input arising from periphery can not reach the cortex through the thalamus [14]. However, thalamo-cortical neurons are depolarized with time by repetitive, synaptic input, and their discharge patterns change from bursting to beating through the resting state. In other words, the role of thalamo-cortical neurons changes from a spindle rhythm generator to a relay station [24,29]. Consequently, the spindle EEG activity disappears, and sensory input can reach the cortex through the thalamus due to an increase in the responsiveness of thalamo-cortical neurons. Therefore, responses of the somatosensory cortex observed in the experiments mainly result from the interaction between the delta rhythm and a periodic ML fiber stimulation.

The response pattern of the somatosensory cortex drifts during a long-lasting periodic ML fiber stimulation: irregular responses → 1:2 phase-locking → 1:1 phase-locking. The spectral peaks of the spontaneous field potential rhythms observed before and after a periodic ML fiber stimulation are 2.8 Hz and 8.6 Hz, respectively. The change of the frequency indicates that the oscillatory state of thalamo-cortical neural networks is changed by the long-lasting ML fiber stimulation. Therefore, even if the frequency of ML fiber stimulation f_i is constant, the frequency ratio f_i/f_o would decrease during a long-lasting stimulation. Since the threshold stimulus current I_{th} also decreases due to temporal summation of synaptic potentials in thalamo-cortical neurons, the normalized stimulus current I/I_{th} relatively increases. Therefore, the drift of the response pattern during a long-lasting periodic ML fiber stimulation would be explained by the drift of the two stimulus parameters, f_i/f_o and I/I_{th}. When the phase diagram in Fig. 8 was obtained the number of current pulses for ML fiber stimulation was limited in order to maintain f_o around 3 Hz. However, if the response pattern depends just on the parameters, f_i/f_o and I/I_{th}, the drift of the response pattern caused by a long-lasting stimulation would be understood as a drift on the phase diagram from lower right to upper left.

The mean response frequency f_r of the field potential in the somatosensory cortex increases with an increase in the stimulus frequency in the regions of phase-lockings. However, the response frequency f_r is limited to about twice as high as the frequency of the spontaneous rhythm due to successive transitions to other phase-locking states, as shown in Fig. 9. Similar experiments have been performed using cortical neurons which respond to a periodic infraorbital nerve stimulation in paralyzed cats [23] and to a periodic mechanical skin stimulation in unanesthetized monkeys [32]. In these experiments, even when the frequency of stimulation is quite high (200 Hz), the mean interspike interval is about 25 ms (40 Hz). In other words, synchronized field potential responses of the cortex caused

by a periodic sensory input would be lower than 40–60 Hz in awaked animals.

Periodic or sustained mechanical movement of vibrissae induces repetitive discharges of neurons in the vibrissa system: the trigeminal ganglions [53], the trigeminal nuclei [41], the thalamus [50], the afferent thalamo-cortical radiation and the cortex [23,42]. Periodic discharges in ML that is a principal path of sensory signals are also caused by a mechanical vibrissa stimulation. Therefore, abscissa of the phase diagram in Fig. 8 may be regarded as the normalized frequency of sensory input from vibrissae to the cortex, and ordinate may be proportional to the number of vibrissae which are simultaneously activated by a mechanical stimulation. Diverse responses shown in the phase diagram would be caused by a natural peripheral stimulation, because the range of the frequency f_i in the present paper corresponds with the frequency range of the activity in the vibrissa system, and several vibrissae are often moved together by a hindrance in the environment. Moreover, if the frequency of spontaneous background rhythm of the cortex varies, the cortex would show different response patterns to the same vibrissa stimulation, because f_i/f_o varies.

If peripheral sensory information is expressed by cortical synchronous oscillations, a wide variety of cortical response patterns would be useful in representing quality and quantity of sensory information. These synchronous oscillations in the cortex may also be caused by input from other parts of the brain. In other words, synchronized oscillations of other neural networks which project to thalamo-cortical networks may substitute for peripheral input and would cause diverse temporal patterns of synchronized oscillations in the sensory cortex. Candidates are the pedunculopontine (PPT), the laterodorsal tegmental (LDT) nuclei [45,46] and the frontal cortex (FC) [26]. Discharge rates of PPT and LDT neurons are about 30 Hz during REM sleep, and the frequency of human magnetic oscillations in FC is 40 Hz during auditory processing [25]. Therefore, interplay of such oscillations and the cortical beta rhythm would result in various synchronized oscillations in the somatosensory cortex which correspond to sensory information. Actually, realistic sensations are often called up, for example, in our dreams, without real sensory input.

It has been found that long term potentiation (LTP) observed in the hippocampus depends on temporal patterns of synaptic input; especially, LTP is facilitated by a burst pattern related to the theta rhythm [38,49]. If LTP in the cortex depends on input patterns as well as in the hippocampus, LTP in the somatosensory association cortex, for example, would depend on the diverse response patterns of the somatosensory cortex shown in this paper, because the response patterns are projected on the association cortex. In other words, the somatosensory cortex would work as a pattern generator, and its diverse synchronized oscillations would be used to control perceptual process and sensory integration in the cortex.

In this paper, it was demonstrated using anesthetized rats that responses of the somatosensory cortex to a periodic ML fiber stimulation are subject to a deterministic law and show a wide variety of oscillatory patterns including chaos. Evidence for chaotic responses was provided by broad band spectra, strange attractors, stretching and folding process, and noninvertible strobomaps with an unstable fixed point. The existence of phase-lockings and chaotic activities in an anesthetized but functional neural network which deals with sensation makes us expect that deterministic activity plays important roles in information processing in the brain. We hope it will be shown in future that primary sensory information is expressed as synchronized temporal patterns, and these patterns are used in the perceptual process.

References

[1] Achermann, P., Hartmann, R., Gunzinger, A., Guggenbühl, W. and Borbély, A.A., All-night sleep EEG and artificial stochastic control signals have similar correlation dimensions, *Electroenceph. Clin. Neurophysiol.*, 90 (1994) 384–387.

[2] Babloyantz, A., Salazar, J.M. and Nicolis, C., Evidence of chaotic dynamics of brain activity during the sleep cycle, *Phys. Lett.*, 111A (1985) 152–156.

[3] Babloyantz, A. and Destexhe, A., Low-dimensional chaos in an instance of epilepsy, *Proc. Natl. Acad. Sci. USA*, 83 (1986) 3513–3517.

[4] Bergé, P., Dubois, M., Manneville, P. and Pomeau, Y., Intermittency in Rayleigh-Bénard convection, *J. Physique-Lettres*, 41 (1980) 341–345.

[5] Bishop, G.H. and O'Leary, J., Components of the electric response to the optic cortex of the rabbit, *Am. J. Physiol.*, 117 (1936) 292–308.

[6] Canavier, C.C., Clark, J.W. and Byrne, J.H., Routes to chaos in a model of a bursting neuron, *Biophys. J.*, 57 (1990) 1245–1251.

[7] Chang H.T., The repetitive discharges of cortico-thalamic reverberating circuit, *J. Neurophysiol.*, 13 (1950) 235–257.

[8] Dvorak, I. and Siska, J., On some problems encountered in the estimation of the correlation dimension of the EEG, *Phys. Lett.*, 118A (1986) 63–66.

[9] Eckhorn, R., Bauer, R., Jordan, W., Brosch, M., Kruse, W., Munk, M. and Reitboeck, H.J., Coherent oscillations: a mechanism of feature linking in the visual cortex, *Biol. Cybern.*, 60 (1988) 121–130.

[10] Eckhorn, R., Frien, A., Bauer, R., Woelbern, T. and Kehr, H., High frequency (60–90 Hz) oscillations in primary visual cortex of awake monkey, *NeuroReport*, 4 (1993) 243–246.

[11] Fell, J., Roeschke, J. and Beckmann, P., Deterministic chaos and the first positive Lyapunov exponent: a non-linear analysis of the human electroencephalogram during sleep, *Biol. Cybern.*, 69 (1993) 139–146.

[12] Frank, G.W., Lookman, T., Nerenberg, M.A.H., Essex, C., Lemieux, J. and Blume, W., Chaotic time series analyses of epileptic seizures, *Physica*, 46D (1990) 427–438.

[13] Freeman, W.J. and Van Dijk B.W., Spatial patterns of visual cortical fast EEG during conditioned reflex in a rhesus monkey, *Brain Res.*, 422 (1987) 267–276.

[14] Glenn, L.L. and Steriade, M., Discharge rate and excitability of cortically projecting intralaminar thalamic neurons during waking and sleep states, *J. Neurosci.*, 2 (1982) 1387–1404.
[15] Grassberger, P. and Procaccia, I., Measuring the strangeness of strange attractors, *Physica*, 9D (1983) 189–208.
[16] Gray, C.M and , König, P., Engel, A.K. and Singer, W., Oscillatory responses in cat visual cortex exhibit intercolumnar synchronization which reflects global stimulus properties, *Nature*, 338 (1989) 334–337.
[17] Hayashi, H., Ishizuka, S., Ohta, M. and Hirakawa, K., Chaotic behavior in the *Onchidium* giant neuron under sinusoidal stimulation, *Phys. Lett.*, 88A (1982) 435–438.
[18] Hayashi, H., Ishizuka, S. and Hirakawa, K., Transition to chaos via intermittency in the *Onchidium* pacemaker neuron, *Phys. Lett.*, 98A (1983) 474–476.
[19] Hayashi, H., Ishizuka, S. and Hirakawa, K., Chaotic response of the pacemaker neuron, *J. Phys. Soc. Jpn.*, 54 (1985) 2337–2346.
[20] Hayashi, H., Ishizuka, S. and Hirakawa, K., Instability of harmonic responses of *Onchidium* pacemaker neuron, *J. Phys. Soc. Jpn.*, 55 (1986) 3272–3278.
[21] Hayashi, H. and Ishizuka, S., Chaotic nature of bursting discharges in the *Onchidium* pacemaker neuron, *J. Theor. Biol.*, 156 (1992) 269–291.
[22] Hayashi, H. and Ishizuka, S., Chaotic responses of the hippocampal CA3 region to a mossy fiber stimulation in vitro, *Brain Res.*, 686 (1995) 194–206.
[23] Hellweg, F.C., Schultz, W. and Creutzfeldt, O.D., Extracellular and intracellular recordings from cat's cortical whisker projection area: thalamocortical response transformation, *J. Neurophysiol.*, 40 (1977) 463–479.
[24] Jahnsen, H. and Llinás, R., Electrophysiological properties of guinea-pig thalamic neurons: an in vitro study, *J. Physiol.*, 349 (1984) 205–226.
[25] Llinás, R.R. and Paré, D., Of dreaming and wakefulness, *Neuroscience*, 44 (1991) 521–535.
[26] Llinás, R.R., Grace, A.A. and Yarom, Y., In vitro neurons in mammalian cortical layer 4 exhibit intrinsic oscillatory activity in the 10- to 50-Hz frequency range, *Proc. Natl. Acad. Sci. USA*, 88 (1991) 897–901.
[27] Lopes da Silva, F.H., Van Rotterdam, A., Storm van Leeuwen, W. and Tielen, A.M., Dynamic characteristics of visual evoked potentials in the dog. II. Beta frequency selectivity in evoked potentials and background activity, *Electroencephalogr. Clin. Neurophysiol.*, 29 (1970) 260–268.
[28] Lopes da Silva, F., Neural mechanisms underlying brain waves: from neural membranes to networks, *Electroencephalogr. Clin. Neurophysiol.*, 79 (1991) 81–93.
[29] McCormick, D.A. and Pape, H.C., Properties of a hyperpolarization-activated cation current and its role in rhythmic oscillation in thalamic relay neurons, *J. Physiol.*, 431 (1990) 291–318.
[30] Morin, D. and Steriade, M., Development from primary to augmenting responses in the somatosensory system, *Brain Res.*, 205 (1981) 49–66.
[31] Morison, R.S. and Dempsey, E.W., The mechanism of thalamocortical augmentation and repetition, *Am. J. Physiol.*, 138 (1942) 297–308.
[32] Mountcastle, V.B., Talbot, W.H., Sakata, H. and Hyvarinen, J., Cortical neuronal mechanisms in flutter-vibration studied in unanesthetized monkeys. Neuronal periodicity and frequency discrimination, *J. Neurophysiol.*, 32 (1969) 452–484.
[33] Osborne, A.R. and Provenzale, A., Finite correlation dimension for stochastic systems with power-law spectra, *Physica*, 35D (1989) 357–381.
[34] Paxinos, G. and Watson, C., *The Rat Brain in Stereotaxic Coordinates*, Academic Press, Sydney, New York, London, 1982.
[35] Perkel, D.H., Schulman, J.H., Bullock, T.H., Moore, G.P. and Segundo, J.P., Pacemaker neurons: effects of regularly spaced synaptic input, *Science*, 145 (1964) 61–63.
[36] Pijn, J.P., Neerven, J.V., Noest, A. and Lopes da Silva, F.H., Chaos or noise in EEG signals; dependence on state and brain site, *Electroencephal. Clin. Neurophysiol.*, 79 (1991) 371–381.
[37] Purpura, D.P., Shofer, R.J. and Musgrave, F.S., Cortical intracellular potentials during augmenting and recruiting responses. II. Patterns of synaptic activities in pyramidal and nonpyramidal tract neurons, *J. Neurophysiol.*, 27 (1964) 133–151.
[38] Rose, G.M. and Dunwiddie, T.V., Induction of hippocampal long-term potentiation using physiologically patterned stimulation, *Neurosci. Lett.*, 69 (1986) 244–248.
[39] Sasaki, K., Staunton, H.P. and Dieckmann, G., Characteristic features of augmenting and recruiting responses in the cerebral cortex, *Exp. Neurol.*, 26 (1970) 369–392.
[40] Segundo, J.P., Altshuler, E., Stiber, M. and Garfinkel, A., Periodic inhibition of living pacemaker neurons. I. Locked, intermittent, messy and hopping behaviors, *Int. J. Bifurc. Chaos*, 1 (1991) 549–581.
[41] Shipley, M.T., Response characteristics of single units in the rat's trigeminal nuclei to vibrissa displacements, *J. Neurophysiol.*, 37 (1974) 73–90.
[42] Simons, D.J., Response properties of vibrissa units in rat somatosensory neocortex, *J. Neurophysiol.*, 41 (1978) 798–820.
[43] Soong, A.C.K. and Stuart, C.I.J.M., Evidence of chaotic dynamics underlying the human alpha-rhythm electroencephalogram, *Biol. Cybern.*, 62 (1989) 55–62.
[44] Steriade, M. and Llinás, R.R., The functional state of the thalamus and the associated neuronal interplay, *Physiol. Rev.*, 68 (1988) 649–742.
[45] Steriade, M., Datta, S., Paré, D., Oakson, G. and Curró Dossi, R., Neuronal activities in brainstem cholinergic nuclei related to tonic activation processes in thalamocortical system, *J. Neurosci.*, 10 (1990) 2527–2545.
[46] Steriade, M., Paré, D., Oakson, G. and Curró Dossi, R., Different cellular types in mesopontine cholinergic nuclei related to pontogeniculo-occipital waves, *J. Neurosci.*, 10 (1990) 2560–2579.
[47] Steriade, M., Gloor, P., Llinás, R.R., Lopes da Silva, F.H. and Mesulam, M.M., Basic mechanisms of cerebral rhythmic activities, *Electroencephalogr. Clin. Neurophysiol.*, 76 (1990) 481–508.
[48] Theiler, J., Spurious dimension from correlation algorithms applied to limited time series data, *Phys. Rev.*, 34A (1986) 2427–2432.
[49] Tsukada, M., Aihara, T., Mizuni, M., Kato, H. and Ito, K., Temporal pattern sensitivity of long-term potentiation in hippocampal CA1 neurons, *Biol. Cybern.*, 70 (1994) 495–503.
[50] Waite, P.M.E., The responses of cells in the rat thalamus to mechanical movements of the whiskers, *J. Physiol.*, 228 (1973) 541–561.
[51] Wang, X.J., Multiple dynamical modes of thalamic relay neuron: rhythmic bursting and intermittent phase-locking, *Neuroscience*, 59 (1994) 21–31.
[52] Wolf, A., Swift, J.B., Swinney, H.L. and Vastano, J.A., Determining Lyapunov exponents from a time series, *Physica*, 16D (1985) 285–317.
[53] Zucker, E. and Welker, W.I., Coding of somatic sensory input by vibrissae neurons in the rat's trigeminal ganglion, *Brain Res.*, 12 (1969) 138–156.